

---

## Active antifungal edible coating based on nanocomposite cast films from galactomannan

---

Gustavo Pereira Gomes de Souza and  
Dirliane do Santos Duarte

Material Science Department,  
Federal University of São Francisco Valley – UNIVASF,  
Petrolina, Brazil  
Email: gustavo.pgsouza@ufpe.br  
Email: dirlianeduarte@gmail.com

Ana Valeria Vieira de Souza,  
Pedro Martins Ribeiro Júnior,  
Maria Auxiliadora Coelho de Lima and  
Douglas de Britto\*

Brazilian Agricultural Research Corporation,  
Embrapa Semiárid,  
BR-428 Highway, Km 152,  
Rural Area – P.O. Box 23, 56302-970,  
Petrolina, PE, Brazil  
Email: ana.souza@embrapa.br  
Email: pedro.ribeiro@embrapa.br  
Email: auxiliadora.lima@embrapa.br  
Email: douglas.britto@embrapa.br  
\*Corresponding author

**Abstract:** Galactomannan is a filmogenic polysaccharide suitable for edible coatings. The addition of nanoencapsulated active ingredients improves its antifungal activity. In this way, nanocomposite materials were developed based on galactomannan and nanoencapsulated essential oil and polyphenols, extracted, respectively from *Lippia grata* and grape skin by-products. The size of chitosan nanoparticles increased after encapsulation, varying from  $42 \pm 24$  to  $295 \pm 0$  nm for polyphenols. Overall, the nanoparticle suspension was stable, with encapsulation efficiency close to 20% for the essential oil and 90% for polyphenols. Nanocomposite films were isolated by casting and characterized by scanning electron microscopy (SEM), infrared spectroscopy (FTIR), water vapour permeability, mechanical properties, release profile, and antifungal activity. By SEM, the films showed good nanoparticle dispersion in the matrix and improved mechanical properties compared to the non-added film. The sample based on essential oil showed good antifungal activity against *Lasiodiplodia theobromae*. Such properties make these films adequate for postharvest coating applications.

**Keywords:** edible film; mesquite gum; essential oil encapsulation; chitosan nanoparticle.

**Reference** to this paper should be made as follows: Gomes de Souza, G.P., do Santos Duarte, D., de Souza, A.V.V., Ribeiro Jr., P.M., de Lima, M.A.C. and de Britto, D. (xxxx) 'Active antifungal edible coating based on nanocomposite cast films from galactomannan', *Int. J. Postharvest Technology and Innovation*, Vol. X, No. Y, pp.xxx–xxx.

**Biographical notes:** Gustavo Pereira Gomes de Souza received his Master's in Materials Science at the Federal University of Vale do São Francisco. He has worked with antifungal coating from polysaccharides.

Dirliane do Santos Duarte is a Master's student in Materials Science at the Federal University of Vale do São Francisco. She has worked with nanotechnology focused on the development and characterisation of nanomaterials and composites.

Ana Valeria Vieira de Souza is a researcher at the Embrapa Semiárid working with plant biotechnology applied to the environment. Her main scientific interests focus on agronomy, with emphasis on plant biotechnology, plant tissue culture, medicinal and aromatic plants, plant genetic resources, plant production, and conservation germplasm.

Pedro Martins Ribeiro Júnior is a researcher at the Embrapa Semiárid working with phytopathology. His research interests are resistance induction, plant-pathogen interaction, and mechanisms involved in the defence response of plants to pathogens.

Maria Auxiliadora Coelho de Lima is a researcher at the Embrapa Semiárid working in the field of agronomy, with emphasis on postharvest physiology and technology. Her current research activities focus on ripening physiology, fruit and vegetable bioactive compounds, postharvest conservation, storage, ripening, ethylene inhibitors, coatings, and shelf life.

Douglas de Britto is currently a researcher at the Embrapa Semiárid working with nanotechnology: development and characterisation of nanomaterial and composites. He has an experience in physical organic chemistry, acting on the synthesis of polysaccharide derivatives such as trimethyl chitosan and carboxymethyl cellulose. He has studied the application of such polymers in postharvest, food, environmental, encapsulation, and controlled release areas, mainly as edible coating, minimally processed fruits, fungicides films, and decontamination of effluents.

---

## 1 Introduction

Fungi cause significant damage to agricultural products and commit billions of economic resources to their control every year. Moreover, fungal mycotoxins can decrease the quality and value of agricultural products and, more importantly, cause injuries or death to animals and humans by ingestion of contaminated products (Khalili et al., 2015).

Several studies have been conducted to reduce such fungal proliferation. Among the various natural substances tested, essential oils (EOs) stand out for their antimicrobial properties both *in vivo* (phytotherapeutic effect) and *in vitro* against an expressive number of fungi, bacteria, viruses, and mites (Cruz-Valenzuela et al., 2013; Bakkali et al., 2008). Particularly in postharvest, the antifungal activity of EO against the fungal genera

*Botrytis*, *Aspergillus*, *Penicillium* and *Alternata* has motivated several studies due to their potential applicability.

The Brazilian semi-arid biome is an important source of EO, featuring several native plant species that produce EO with antimicrobial activity, e.g., *Lippia grata* (Souza et al., 2017). The antifungal activity of the EO of *Lippia* ssp. has already been verified against common postharvest fungi (Carvalho et al., 2013), specially against *Lasiodiplodia theobromae* (Peixinho et al., 2017).

Polyphenols (PPh) are another substance that can also be used as antimicrobials, being found in large quantities as winery by-products. Likewise, some PPh have shown antifungal activity and aroused the interest of the postharvest sector (Friedman, 2014).

However, both EO and PPh may lose their activity depending on how they are processed. EO is volatile compounds and can be easily degraded when composing manufactured formulations. Different strategies can increase their activity and stability, such as nanoencapsulation (Kedia and Dubey, 2018). Similarly, the biological activity of PPh may depend on the form of their administration, and nano-sized carriers can be applied to improve their activity (Liang et al., 2011).

Some polysaccharides, such as chitosan, mainly due to their chelating and cross-linking properties, can be used to encapsulate active compounds, with direct applications in postharvest areas (Picard et al., 2013; Sae-Tang et al., 2020). Particularly in the food segment, the water-soluble vitamins C, B9, and B12 have been successfully encapsulated in chitosan nanoparticles (NP) (Britto et al., 2012). In a subsequent study, it was found that the encapsulation efficiency (EE) is dependent on the structure of the nanoparticle as well as the solubility of the vitamin in the reaction medium (Britto et al., 2014). Chitosan has also been used to encapsulate EO (Hadidi et al., 2020; Hosseini et al., 2013) and PPh (Liang et al., 2011).

Another particularly important property of polysaccharides in postharvest studies is their film-forming ability, constituting the basis of the formulation of edible coatings (Nascimento et al., 2019). Galactomannan is an interesting polysaccharide with filmogenic properties, being found in the mesquite seed gum (*Prosopis juliflora*), a very common tree in the Brazilian Northeast region (Cerqueira et al., 2011). This application represents a potential and low-cost alternative for exploiting this species classified as invasive in the Caatinga biome.

The combination of filmogenic polysaccharides with NP containing nanoencapsulated active ingredients generates nanocomposite (NC) films with potential application for coating fruits and vegetables. This is an important alternative to extend the shelf-life of perishable tropical fruits such as mango, for example (Medeiros et al., 2012).

From this perspective, the present study aimed to prepare and characterise films in terms of composition, morphology, mechanical properties, water vapour permeability, and release of active ingredients aiming at their application as active coatings in mango. The films consisted of a polymeric matrix of galactomannan (GLM) extracted from the mesquite seed (*Prosopis juliflora*) combined with encapsulated chitosan NP with active ingredients. The active ingredients were the EO of *Lippia grata* and PPh extracted from the grape skin by-product.

## 2 Materials and methods

### 2.1 Materials

Sodium tripolyphosphate (TPP) and medium molecular weight chitosan (80% deacetylation degree) were purchased from Aldrich Chemical Company Inc. (USA). Ethanol (99.8% pure) and glacial acetic acid were purchased from Dinâmica (Brazil). The other reagents were purchased from Synth (Brazil).

The EO was extracted from *Lippia grata* leaves collected from the Caatinga experimental field of Embrapa Semiárid. The leaves were oven-dried (30°C) and subjected to hydrodistillation in a Clevenger apparatus. The PPh were obtained from the hydroalcoholic extract of grape skin by-products (*Vitis vinifera* variety Egidolla). Galactomannan (GLM) was extracted from mesquite tree seeds. For this, the seeds were crushed, extracted with hot water (50°C), and centrifuged at  $12,857 \times g$  (centrifuge Eppendorf, model 5804 R, rotor F-34-6-38, 10,000 rpm) for 15 minutes and 20°C to separate the non-dissolved residue. Subsequently, the GLM was precipitated with ethanol and isolated by lyophilisation (−50°C, 200 µHg) in an equipment from LioBras® model L101 (Souza Filho et al., 2013).

### 2.2 Preparation of the encapsulated nanoparticles and NC films

The NP were prepared by ionic gelation process, following the procedure described previously (Britto et al., 2012, 2014) with some modifications. Initially, a solution with  $3.0 \text{ mg mL}^{-1}$  chitosan was prepared in 0.5% aqueous acetic acid and kept under magnetic stirring at room temperature for 24 hours. Subsequently, a solution with  $1.6 \text{ mg mL}^{-1}$  TPP in 0.5% aqueous acetic acid was prepared under magnetic stirring for 10 mins at room temperature. NP formation by ionic gelation was performed by adding 50 mL of the TPP solution to 50 mL of the aqueous chitosan solution at a rate of  $1 \text{ mL min}^{-1}$  at room temperature and under magnetic stirring. The NP suspension was then centrifuged at  $35,392 \times g$  (centrifuge Beckman Coulter, model Avanti J26-XP, rotor JA 25.15, 20,000 rpm) for 20 minutes at 8°C to obtain the NP precipitate.

For the encapsulation process, the active substances (EO or PPh) were previously dissolved in 2.5 mL of an ethanol-water solution (1:1 v/v) at a concentration of  $32 \text{ mg mL}^{-1}$ . In parallel, the NP precipitate was re-suspended in 2.5 mL of ethanol-water solution (1:1 v/v). Subsequently, the solution with the active substance was mixed with the NP suspension in an ultrasonic bath (Ultrasonic Cleaner®, model PS-20, ultrasonic power 100 W) for 10 minutes to obtain 5.0 mL of encapsulated substance. The NP samples were named NP-EO and NP-PPh for encapsulation with EO and PPh, respectively. For the non-encapsulated sample, the NP precipitate was resuspended in a similar way, except the addition of the active substance. The sample was named NP-Ch.

Finally, the NC film was obtained by adding the 5.0 mL of the encapsulated NP suspension to a GLM solution dissolved in water to obtain a final volume of 60 mL and a GLM concentration of  $5 \text{ mg mL}^{-1}$ . The NC were then prepared by casting in three 20 mL Petri dishes (diameter = 90 mm) at room temperature. The NC samples were named NC-EO, NC-PPh and NP-Ch, respectively for samples added with NP-EO, NP-PPh and NP-Ch.

### 2.3 *EE and controlled release from the encapsulated nanoparticles*

The NP synthesis was performed as described above and the encapsulation was performed as follows. The centrifuged NP were re-suspended in 1:1 ethanol-water or deionised water and placed to interact with EO and PPh solutions at four different concentrations (8.0, 4.0, 2.24, and 0.8 mg mL<sup>-1</sup>) with the aid of an ultrasonic bath (Ultrasonic Cleaner<sup>®</sup>, model PS-20, ultrasonic power 100 W) for 80 minutes (three cycles of 20 minutes with a 10-minute interval between them). After the interaction, the encapsulated NP suspension was centrifuged and the supernatant quantified by UV-visible spectrophotometry using a Thermo Scientific<sup>®</sup> spectrophotometer, model MultiSkan GO. A previous calibration curve was done with adequate concentrations of EO and PPh.

The NP precipitate was analysed for controlled release. For this, 1.0 g of the NP precipitate was placed in amber glass flasks along with 24 mL phosphate buffer (Na<sub>2</sub>HPO<sub>4</sub> and KH<sub>2</sub>PO<sub>4</sub>) and 16 mL ethanol, totalling 40 mL of solution. The system was placed on an orbital shaker at 120 rpm and 25°C. Aliquots (1.5 mL) were withdrawn at pre-determined time intervals up to 24 hours, centrifuged at 12,857 × g (centrifuge Eppendorf, model 5804R, rotor F-34-6-38, 10,000 rpm, 10 mins, 9°C), and quantified by UV-visible spectroscopy as described above. The experiment was performed in triplicate.

### 2.4 *Morphology*

For the morphological analysis, the NP suspensions were deposited on glass slides and evaluated under scanning electron microscopy (SEM) using a Tescan Vega 3 microscope (Brno, Czech Republic). Electrical conductivity was assessed by applying a thin coating layer of gold and silver paint in the lateral part of the glass slides. It was analysed at least two replication for each sample.

### 2.5 *Nanoparticles size and zeta potential*

The size and zeta potential of the nanoparticles (NP-EO, NP-PPh, and NP-Ch) were evaluated using the dynamic light scattering (DLS) technique in a Zetasizer Nano ZS Zen 3600 equipment from Malvern Instruments Ltd. (England). All analyses were performed in triplicate at 25°C.

### 2.6 *Fourier-transform infrared spectroscopy*

The spectra of the NC films were obtained using a Fourier-transform infrared spectroscopy (FTIR) equipment from Perkin Elmer, model spectrum two (Waltham, MA, USA), in the range of 4,000–400 cm<sup>-1</sup> wave numbers, with eight cumulative scans.

### 2.7 *Mechanical properties*

Due to the fragile nature of the films, it was necessary to follow the methodology described by Talucdher and Shivakumar (2013). The paper mould used measured 38 × 25 mm with a central opening of 6 × 12 mm. The sample consisted of a rectangular film measuring 5 × 15 mm and with thickness ranging from 0.016 mm to 0.028 mm. The

stress × strain curve was obtained with a universal testing machine (EMIC, DL 10000, Paraná, Brazil). The cell load was 500 N, with a deformation speed of 5 mm min<sup>-1</sup>. The experiment was repeated at least six times for each sample.

### 2.8 Water vapour permeability

Water vapour permeability was determined by gravimetry, according to the ASTM standard test methods (ASTM E96/E95M, 1995). For this, disc-shaped sample film pieces with a diameter of 30 mm were attached to the measuring cells containing 20 mL of water. The cells were placed in a desiccator containing silica gel at 50% relative humidity. Each cell was weighed on an analytical balance for seven days. The experiment was performed in triplicate, and permeability was calculated using equation (1):

$$PVA = \frac{\Delta ME}{TAS(R_1 - R_2)} \quad (1)$$

where 'PVA' is the water vapour permeability (g·mm/kPa·h·m<sup>2</sup>); 'ΔM' is the change in mass (g) of the cell; 'E' is the average thickness (mm) of the film; 'T' is the time (hours); 'A' is the permeation area (m<sup>2</sup>) of the film; 'S' is the water vapour pressure (3.2 kPa) at the test temperature (25°C); 'R<sub>1</sub>' is the relative humidity within the cell, expressed as a fraction (1.0); and 'R<sub>2</sub>' is the relative humidity in the desiccator, expressed as a fraction (0.5).

### 2.9 Release profile from the NC films

The release profile was performed for NC-EO, NC-PPh and NP-Ch films. For this, the NC were prepared as described above, except that they were dried by lyophilisation to avoid possible degradation of the EO or polyphenols. In this way, the NC samples were placed on Petri dishes, frozen at -80°C, and subsequently lyophilised (-50°C, 200 μHg) in an equipment from LioBras<sup>®</sup> model L101. After drying, the release profile for NC films was done as described above for NP. For this, approximately 100 mg of the sample was used in 15 mL of the released solution (60% ethanol and 40% phosphate buffer). Aliquots of 1.0 mL were withdrawn after 0.5, 1.0, 2.0, 3.0, 5.0, and 24 hours. Subsequently, the aliquots were centrifuged to separate the solid particles. The supernatant was diluted with 4 mL of ethanol-water solution (1:1) and analysed in a Thermo Scientific<sup>®</sup> UV-visible spectrophotometer, as described above. The experiment was performed in triplicate.

### 2.10 In vitro test against *Lasiodiplodia theobromae*

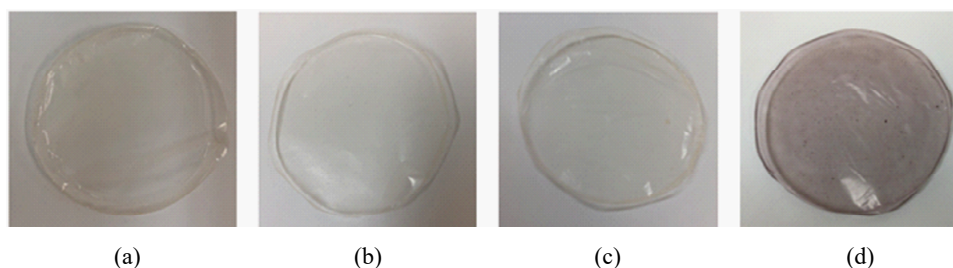
The antifungal activity of the EO of *L. grata* was evaluated against *Lasiodiplodia theobromae* by spreading 200 μL of the NC film formulation over 9 cm-diameter Petri dishes containing PDA medium (potato, dextrose, and agar) with a Drigalski loop. The samples were then transferred to a laminar flow chamber for sterilisation with UV light for 15 minutes. After this period, a 5 mm mycelium disk of the fungus *L. theobromae* was placed at the centre of the plate. After three days of incubation at 25°C and with a 12-hour photoperiod, colony diameter was evaluated with the aid of a calliper.

The experiment was conducted in a completely randomised experimental design with four replications, with each plot represented by one Petri dish. The means were subjected to analysis of variance and compared by the Tukey test when significant by the F test ( $P \leq 0.05$ ).

### 3 Results and discussion

The films with the polymeric GLM matrix at a concentration of  $5 \text{ mg mL}^{-1}$  showed good filming-forming ability. The films were homogeneous and showed slightly yellowish tones, except for the purple tone observed in the films with PPh (Figure 1). Such lighter tones provide a better aesthetic advantage for fruit coating, with little interference in fruit colour.

**Figure 1** Typical aspect of the films obtained with, (a) parent galactomannan (GLM) and galactomannan NC charged with (b) non-encapsulated chitosan nanoparticle (NC-Ch) (c) chitosan nanoparticle encapsulated with *Lippia grata* EO (NC-EO) (d) chitosan nanoparticle encapsulated with grape skin polyphenols (NC-PPh) (see online version for colours)



Note: The films diameter is approximately 90 mm.

#### 3.1 EE and controlled nanoparticle release

The EE evaluation showed that the EE value obtained for encapsulation in water medium (NP-EO<sub>wt</sub>), for all the concentrations tested, was higher than EE in ethanol medium (NP-EO<sub>et</sub>, Table 1). However, the aspect of the NP-EO<sub>wt</sub> sample was not homogeneous, forming agglomerates and precipitating spontaneously. On the other hand, the NP-EO<sub>et</sub> sample showed a more homogeneous aspect in suspension and did not precipitate. This result suggests an unstable system for the NP-EO<sub>wt</sub> sample probably caused by the difference in solubility between the EO and water. This clearly evidences that the EE value, for a general system, is function of the solvent used and chemical property of the encapsulated substance rather than the NP structure itself (Britto et al., 2012, 2014). Considering all this aspects, the NP-EO<sub>wt</sub> was rejected and the NP-EO<sub>et</sub> elected for the subsequent study, even with a lower EE value in comparison with NP-EO<sub>wt</sub>.

The initial concentration of the active ingredient also plays an important role in the EE (Table 1). The EE clearly showed greater efficiency at higher initial concentrations of EO. Clove EO in aqueous emulsion containing surfactant was encapsulated in chitosan nanoparticles, resulting in a maximum EE of approximately 46% (Hasheminejad et al., 2019). In another study, the EO of *Lippia menosides* was also encapsulated in chitosan

nanoparticles using a surfactant, resulting in a maximum EE of 69% (Paula et al., 2010). In both studies cited, the EE decreased when high oil concentrations were added to the system, probably due to a possible saturation of chitosan when encapsulating all the material. However, these literature data are based on a complex procedure, with two-step approach or additional spray-drying technique.

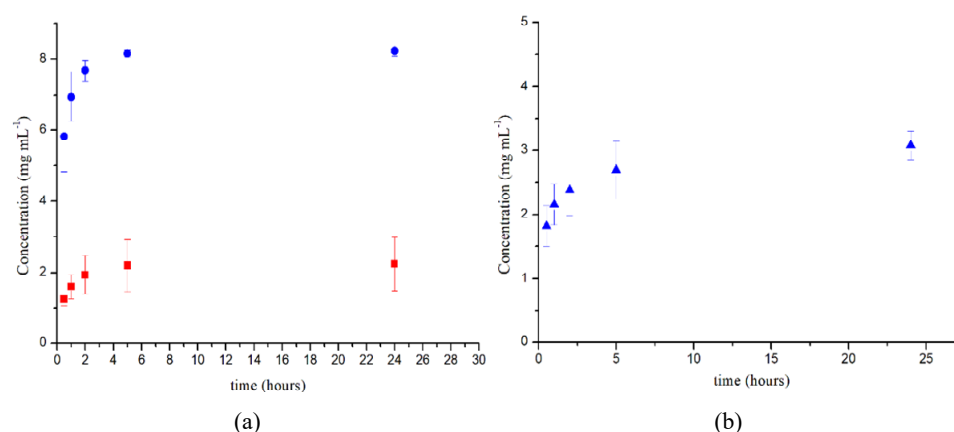
**Table 1** Initial concentration ( $C_i$ , mg mL<sup>-1</sup>), final concentration ( $C_f$ , mg mL<sup>-1</sup>) and EE (EE, %) for loading chitosan nanoparticles with *Lippia grata* EO in ethanol-water 1:1 (NP-EO<sub>et</sub>) and water (NP-EO<sub>wt</sub>) media and with polyphenols from grape skin in ethanol-water 1:1 medium (NP-PPh<sub>et</sub>)

NP-EO <sub>et</sub>			NP-EO <sub>wt</sub>			NP-PPh <sub>et</sub>		
$C_i$	$C_f$	EE	$C_i$	$C_f$	EE	$C_i$	$C_f$	EE
8.0	6.5	19.0	8.0	2.5	69.1	8.0	0.5	93.1
4.0	3.2	21.2	4.0	1.9	53.6	4.0	0.4	89.9
2.24	1.9	13.6	2.24	1.5	32.2	2.24	0.2	90.6
0.8	0.76	5.6	0.8	0.65	18.4	0.8	0.04	93.9

The efficiency of the NP-PPh sample was very high, showing little dependence on the initial concentration. Liang et al. (2011), encapsulated green tea polyphenols in chitosan nanoparticles obtained a maximum EE of around 83%.

The release profile for the NP-EO<sub>wt</sub> sample in phosphate buffer-ethanol solution showed an initial burst release and reached a plateau at 8.21 mg mL<sup>-1</sup> (Figure 2). The profile of NP-EO<sub>et</sub> (Figure 2) was similar, but the plateau was reached at a lower concentration (2.8 mg mL<sup>-1</sup>) (Britto et al., 2014). Such a difference is related to the EE discussed before. The NP-EO<sub>wt</sub> sample had more EO than the NP-EO<sub>et</sub> sample, although not effectively encapsulated in the chitosan nanoparticles. The release profile for the NP-PPh<sub>et</sub> sample was similar to the NP-EO<sub>et</sub> sample, reaching a plateau at 3.0 mg mL<sup>-1</sup>.

**Figure 2** Release profile (average  $\pm$  SD) for chitosan nanoparticle loaded with, (a) *Lippia grata* EO obtained from water medium (●) and ethanol-water medium (■) (b) load with grape skin polyphenols obtained from ethanol-water medium (▲) (see online version for colours)



Note: The releasing solution was phosphate buffer (Na<sub>2</sub>HPO<sub>4</sub> and KH<sub>2</sub>PO<sub>4</sub>): ethanol.

### 3.2 Nanoparticle size and zeta potential

The particle size and zeta potential are important considerations when designing a delivery system for bioactive compounds. In theory, NPs should ideally have the smallest possible size and the greatest zeta potential. Uniformity in nanoparticle size distribution is crucial to maintain a constant release rate of the encapsulated material (Bulmer et al., 2012; Barzegar et al., 2016). Furthermore, high zeta potential values ensure the stability of the dispersed nanoparticles.

The NP-Ch samples showed a zeta potential close to +30 mV (Table 2), indicating a highly stable suspension (Lorevice et al., 2016). As chitosan was solubilised in acetic acid, the amine groups ( $\text{NH}_2$ ) were ionised into ionic  $\text{NH}_3^+$  groups, causing the positive zeta potential values observed here (Britto et al., 2014; Antoniou et al., 2015; Gan and Wang, 2007).

**Table 2** Zeta potential values (mV) for the non-encapsulated chitosan nanoparticles (NP-Ch); chitosan nanoparticles encapsulated with *Lippia grata* essential oil (NP-EO) and chitosan nanoparticles encapsulated with grape skin polyphenols (NP-PPh)

Sample	Zeta potential
NP-Ch	$28.0 \pm 0.1$
NP-EO	$8.2 \pm 0.1$
NP-PPh	$14.2 \pm 0.4$

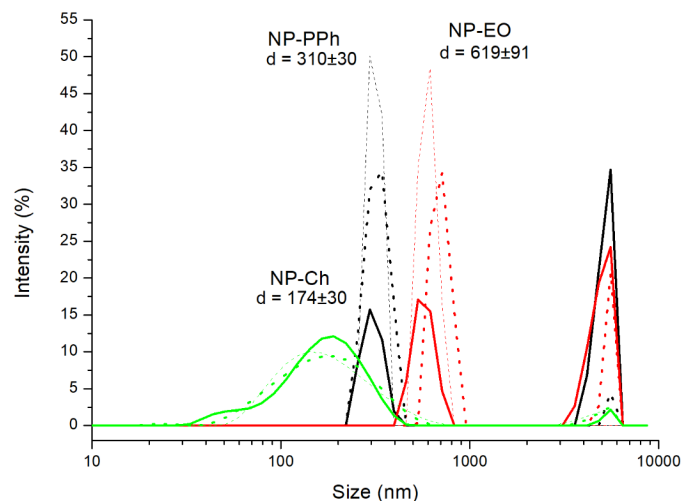
The zeta potential showed a sharp decrease for the encapsulated systems compared to the non-encapsulated system (Table 2). In fact, the zeta potential is greatly influenced by the encapsulated substance (Britto et al., 2014). Despite the positive character of chitosan nanoparticles, Paula et al. (2010) found negative values for chitosan nanoparticles incorporated with the essential oil of *Lippia ssp.* Therefore, the decrease in the zeta potential of NP-EO and NP-PPh can be attributed to a possible negative character of those substances.

Regarding the size, all samples showed a peak around 5,500 nm, according to the DLS graph of intensity versus particle size (Figure 3). Such peaks are indicative of clusters formation (Britto et al., 2012). Hydrogel nanoparticles such as chitosan-TPP show high interaction with the aqueous solvent, facilitating the formation of clusters. This also influences the process of nanoparticle isolation, forming clusters of nanoparticles in the solid state (Silva et al., 2020). This cluster formation can be increased depending on the chemical nature of the encapsulated substance. The increase in intensity in this region is indicative that this phenomenon is occurring with the NP-EO and NP-PPh samples (Figure 3). In accordance, the non-encapsulated sample, NP-Ch, showed the lowest nanoparticle size,  $174 \pm 30$  nm, followed by NP-PPh, with  $310 \pm 30$  nm, and finally by NP-EO,  $619 \pm 91$  nm, with the largest value (Figure 3).

The DLS graph of particle number versus size gives a better idea of the characteristics of nanoparticles (Figure 4). According to the graph, the absolute number of nanoparticles in the 5,500 nm range is very low, indicating that the formation of these clusters is also very low compared to the other ranges. The size distribution trend followed the same observed for intensity, although with lower values. The non-encapsulated sample, NP-Ch, showed the lowest nanoparticle size,  $42 \pm 24$  nm, followed by NP-PPh, with  $295 \pm 0$  nm, and finally by NP-EO, with  $603 \pm 67$  nm, the largest value (Figure 4). This size

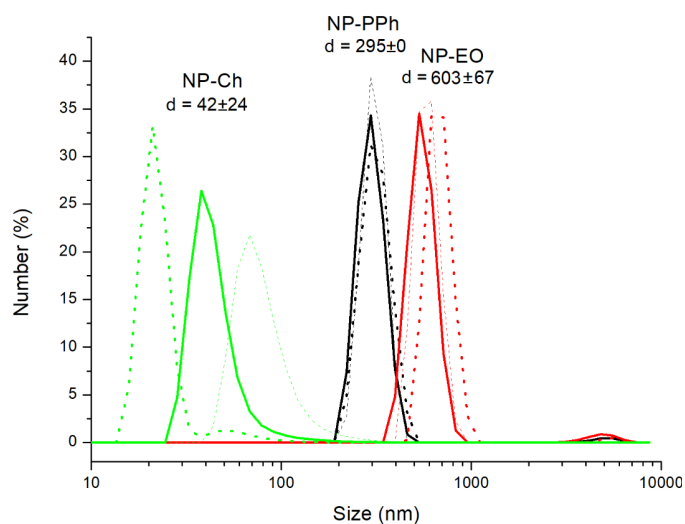
distribution for NP-Ch agrees with the literature (Britto et al., 2014; Otoni et al., 2014). Furthermore, there is an increase in nanoparticle size usually after the encapsulation process (Britto et al., 2012, 2014; Kavaz et al., 2019).

**Figure 3** DLS graph of intensity versus particle size for the non-encapsulated chitosan nanoparticles (NP-Ch); chitosan nanoparticles encapsulated with *Lippia grata* essential oil (NP-EO) and chitosan nanoparticles encapsulated with skin grape polyphenols (NP-PPh) (see online version for colours)



Note: Different line style stands for triplicate analysis.

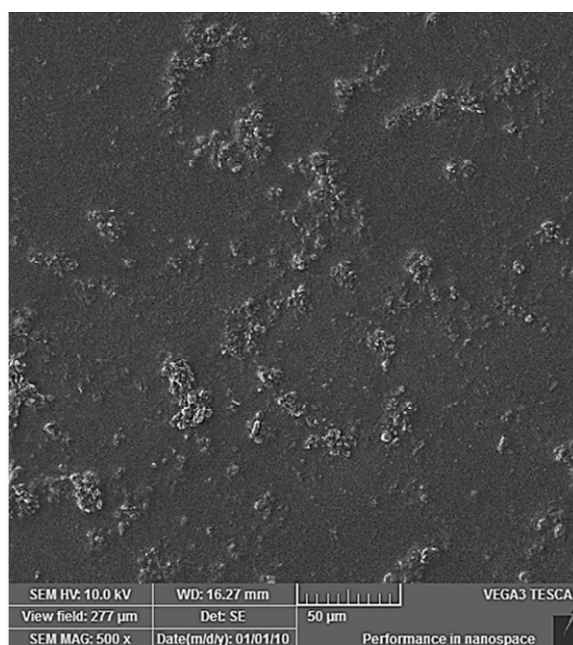
**Figure 4** DLS graph of number versus particle size for the non-encapsulated chitosan nanoparticles (NP-Ch); chitosan nanoparticles encapsulated with *Lippia grata* essential oil (NP-EO) and chitosan nanoparticles encapsulated with skin grape polyphenols (NP-PPh) (see online version for colours)



### 3.3 NC morphology

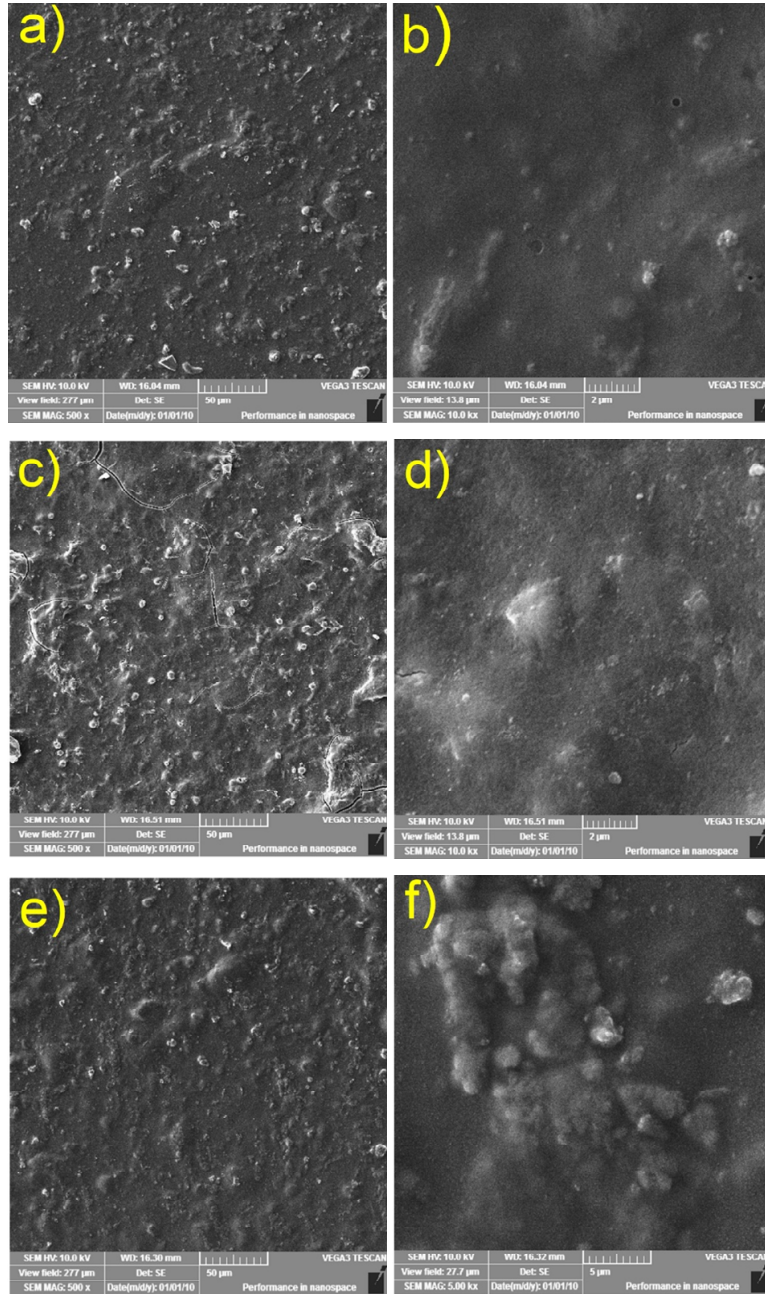
The parent GLM film (without NP addition) showed an irregular surface with several spherical structures evenly distributed (Figure 5). Such structures have been reported before and may be related to the formation of a colloidal system expected to occur during film casting (Nascimento et al., 2019).

**Figure 5** SEM image for galactomannan film cast on glass sheet at 500 x magnification



After the addition of nanoparticles, the SEM images of the NC-Ch, NC-EO, and NC-PPh samples showed increased irregularities (Figure 6) compared to the parent sample (Figure 5). This accounts for the regular distribution of the nanoparticles in the GLM matrix. Spherical structures with different diameters can be seen in the images with 500 x magnification [Figures 6(a), 6(c) and 6(e)]. Large structures ( $d \sim 5,000$  nm) may result from the formation of clusters during the casting process. In fact, chitosan nanoparticles are expected to be highly miscible within GLM matrix due to their similar chemical aspect (polysaccharide-polyelectrolyte-TPP) and the low viscosity of the solution (Duarte et al., 2019). However, as pointed above, the hydrogel character may favour this cluster formation in the solid state after casting. On the other hand, small structures ( $d < 5,000$  nm) can be seen embedded in the galactomannan matrix [Figures 6(a), 6(c) and 6(e)], in accordance with what was described before (Nascimento et al., 2019). In high-magnification images (5.0–10.0 kx), spherical structures can be seen in the range of  $d = 200 - 500$  nm, mainly for NC-Ch and NC-PPh [Figures 6(b) and 6(d)]. On the other hand, such structures are not clearly defined in the NC-EO sample [Figure 6(f)]. This may occur due to two reasons: first, the NP-EO showed the largest nanoparticle size, and second, the hydrophobic character of the essential oil may favour the formation of clusters during casting (Hadidi et al., 2020).

**Figure 6** SEM images for galactomannan NC films cast on glass sheet, containing the addition of. (a)–(b) non-encapsulated chitosan nanoparticles (NC-Ch) (c)–(d) chitosan nanoparticles encapsulated with skin grape polyphenols (NC-PPh) (e)–(f) chitosan nanoparticles encapsulated with *Lippia grata* essential oil (NC-EO) at different magnifications (a) (c) (e) 500 x (b) (d) 10.0 kx (f) 5.0 kx (see online version for colours)



### 3.4 Mechanical properties of the NC films

The addition of the nanoparticles to the GLM matrix resulted in more resistant NC films (NC-Ch and NC-PPh) compared to the parent GLM film (Figure 7 and Table 3). On the other hand, the NC film incorporated with NP-OE did not show any improvements in its mechanical properties. Generally, the addition of nanostructures to the polysaccharide matrix produces NC films with improved physical properties, leading to increased tensile strength and maximum deformation (Antoniou et al., 2015; Azeredo, 2009; Lu et al., 2005). In the case of NC-EO films, the decrease in tensile strength can be attributed to the free essential oil that volatilised, leaving void areas in the material. The literature also reports a plasticising effect of EOs in edible films demonstrated by the reduced strength and stiffness while increasing film elongation (Otoni et al., 2014).

**Figure 7** Stress-strain deformation behaviour (average  $\pm$  SD) for parent GLM (■) and galactomannan NCs films charged with non-encapsulated chitosan nanoparticles (●), nanoparticles encapsulated with grape skin polyphenols (▲) and nanoparticles encapsulated with *Lippia grata* essential oil (★) (see online version for colours)

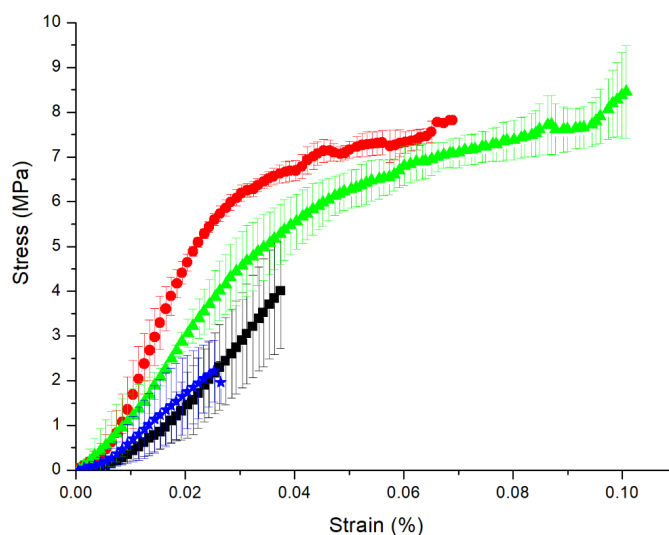


**Table 3** Tensile strength (MPa) and maximum deformation yield (%) parameters according the stress-strain deformation behaviour for galactomannan film (GLM) and galactomannan NCs films charged with non-encapsulated chitosan nanoparticles (NC-Ch); chitosan nanoparticles encapsulated with grape skin polyphenols (NC-PPh) and chitosan nanoparticles encapsulated with *Lippia grata* essential oil (NC-EO)

Sample	Tensile strength	Maximum deformation
NC-EO	$2.6 \pm 0.4^a$	$3.2 \pm 0.8^a$
GLM	$3.7 \pm 0.1^a$	$3.6 \pm 0.7^a$
NC-Ch	$7.4 \pm 0.5^{bc}$	$6.6 \pm 0.7^b$
NC-PPh	$8.7 \pm 2.1^c$	$11.2 \pm 3.3^c$

Note: Different letters in columns indicate that the means difference is significant at the 0.05 level Tukey test.

### 3.5 Water vapour permeability through the NC films

The addition of nanoparticles to the GLM matrix did not result in improved water vapour permeability for NC-Ch and NC-PPh compared to the parent GLM film (Table 4). On the other hand, despite the hydrophobic character of the EO, the NC film incorporated with NP-OE showed increased water vapour permeability. This may be related to the same phenomenon described above for the decrease in the mechanical properties. Void areas caused by essential oil volatilisation facilitated water vapour diffusion through the film.

**Table 4** Water vapour permeability  $[(\text{g}\cdot\text{mm})\cdot(\text{kPa}\cdot\text{h}\cdot\text{m}^2)^{-1}]$  for GLM and galactomannan NCs films charged with non-encapsulated chitosan nanoparticles (NC-Ch); chitosan nanoparticles encapsulated with grape skin polyphenols (NC-PPh) and chitosan nanoparticles encapsulated with *Lippia grata* essential oil (NC-EO)

Sample	WVP
NC-EO	$0.374 \pm 0.009^{\text{a}}$
NC-Ch	$0.225 \pm 0.024^{\text{bc}}$
NC-PPh	$0.227 \pm 0.004^{\text{cd}}$
GLM	$0.194 \pm 0.022^{\text{d}}$

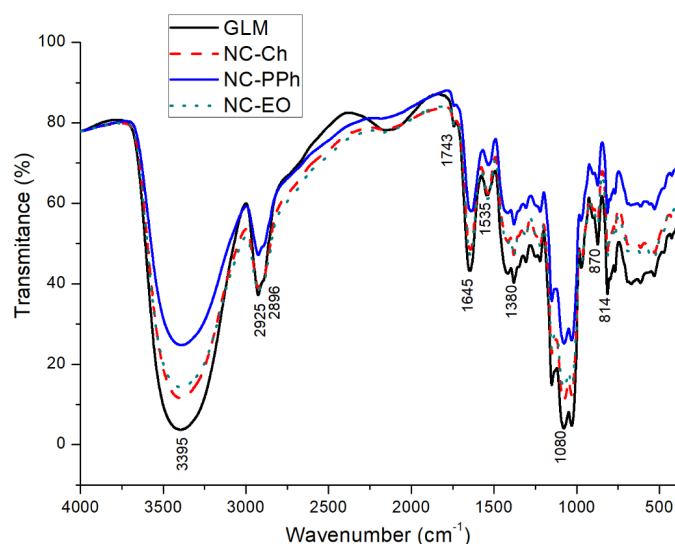
Note: Different letters in columns indicate that the means difference is significant at the 0.05 level Tukey test.

### 3.6 Infrared spectroscopy (FTIR) of the NC films

The FTIR spectrum of the GLM cast film showed typical bands of polysaccharide galactomannan (Figure 8). The most relevant ones are the bands at  $3,395\text{ cm}^{-1}$  (axial deformation of OH);  $2,925$  and  $2,896\text{ cm}^{-1}$  (axial deformation of  $\text{CH}_2$  and  $\text{CH}$ , respectively);  $1,380\text{ cm}^{-1}$  (angular deformation on the plane of OH); and  $1,080\text{ cm}^{-1}$  (axial deformation of CO, COC), which are characteristic of gluco-polysaccharides and have been previously described in the literature (Cerqueira et al., 2012). Particularly for galactomannans, the bands at  $860$  and  $814\text{ cm}^{-1}$  are related to the presence of anomeric configurations ( $\alpha$  and  $\beta$  conformers) and glycosidic linkages attributed to  $\alpha$ -D-galactopyranose and  $\beta$ -D-mannopyranose units, respectively (Nascimento et al., 2019; López-Franco et al., 2013). Bands at  $1,743$ ,  $1,645$ , and  $1,535\text{ cm}^{-1}$  were also found (attributed, respectively, to C=O in carboxylic acid, C=O in amide and N-H) and may be related to the presence of proteinaceous contaminants (López-Franco et al., 2013).

The addition of nanoparticles did not cause changes in the GLM FTIR spectra (Figure 8). The most relevant change is related to the O-H absorption band, which decreased for the NCs, with NC-PPh showing the greatest decrease. It is not possible to state what phenomenon was responsible for this decrease, although it may be related to the amount of absorbed  $\text{H}_2\text{O}$  or the reduction of intermolecular hydrogen bonds. Chitosan shows characteristic bands close to  $1,500$ – $1,600\text{ cm}^{-1}$  (Nascimento et al., 2019). As well, the formation of NP structure implies in changes in the FTIR spectrum, mainly at  $2,120\text{ cm}^{-1}$  referent to chitosan ammonium ion (Britto et al., 2012). However, the mass proportion for GLM and NP is high, resulting in overlapping of such characteristic bands by the GLM one.

**Figure 8** FTIR spectra for GLM and galactomannan NC films charged with non-encapsulated chitosan nanoparticles (NC-Ch); chitosan nanoparticles encapsulated with grape skin polyphenols (NC-PPh) and with chitosan nanoparticles encapsulated with *Lippia grata* essential oil (NC-EO) (see online version for colours)



### 3.7 Release profile from the NC films

The release profile of the EO and PPh from the NC was similar to that observed for encapsulated nanoparticles (Figure 9), reaching a plateau after up to five hours. These results characterise a good prolonged release profile required for postharvest applications, in which the active ingredient must be gradually released on the fruit surface for as long as possible.

The release of active substances from nanoparticles occurs through several mechanisms, including surface erosion, disintegration, diffusion, and desorption (Hosseini et al., 2013). The release profile of the EO and PPh from the nanoparticles within the GLM matrix can be described as a two-stage process. Initially, a high release rate occurs, then followed by a subsequent slower release. The high initial release can be attributed to the active ingredient molecules adsorbed on the surface of the particles, which are quickly released to the solvent (Britto et al., 2014; Hosseini et al., 2013).

### 3.8 *In vitro* test against *Lasiodiplodia theobromae*

The *in vitro* test demonstrated the antifungal activity of the NC-EO sample against the fungus *L. theobromae* (Figure 10). This sample showed a more restricted development in mycelial diameter compared to the control [Figure 10(a)]. The NC with non-encapsulated nanoparticles (NC-Ch) and the parent galactomannan film (GLM) did not show antifungal activity. The GLM film without UV-visible radiation pre-treatment showed some apparent antifungal activity. However, after the UV-visible radiation pre-treatment, the GLM barely showed any activity. This may occur due to contaminants present in the non-treated GLM, which reduced the mycelium spread.

**Figure 9** Release profile (average  $\pm$  SD) for galactomannan NC film charged with chitosan nanoparticle encapsulated with *Lippia grata* essential oil (■) and grape skin polyphenols (●) in a phosphate buffer ( $\text{Na}_2\text{HPO}_4$  and  $\text{KH}_2\text{PO}_4$ ) – ethanol releasing media solution (see online version for colours)

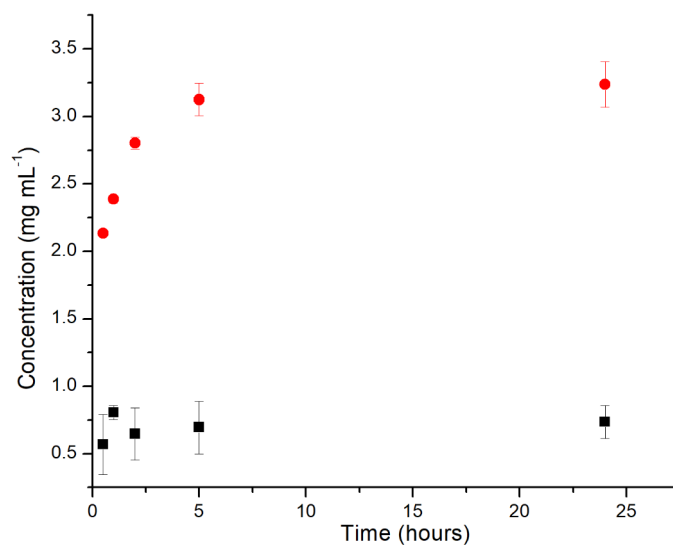
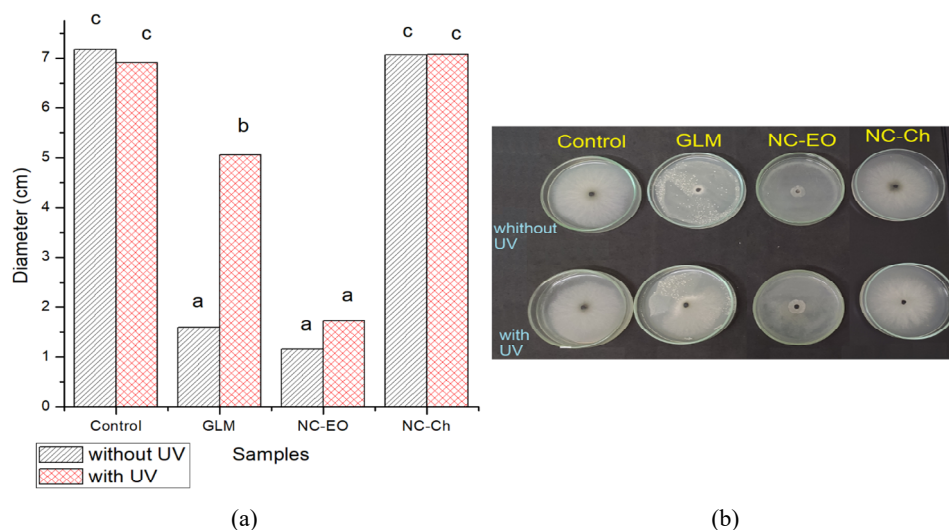


**Figure 10** (a) Antifungal activity against *Lasiodiplodia theobromae* in function of diametrical mycelia development for galactomannan cast film (GLM) and galactomannan NCs films charged with non-encapsulated chitosan nanoparticles (NC-Ch) and chitosan nanoparticles encapsulated with *Lippia grata* essential oil (NC-EO) (b) Mycelia spread typical aspect after three days of incubation (see online version for colours)



Note: Different letters in columns indicate that the means difference is significant at the 0.05 level Tukey test.

Most essential oils have activity against fungi and bacteria due to the presence of monoterpenes. Specifically, in the EO of *L. grata*, the main constituents are carvacrol and

thymol, classified as phenolic monoterpenes (Souza et al., 2017). The mechanisms of action of essential oils on microorganisms are known to modify the cell membrane structure, causing the breakdown of the intracellular nucleic acid and the inactivation of some fundamental enzymes (Albuquerque et al., 2006).

#### 4 Conclusions

The active ingredient composed of polyphenols from grape skins was more efficiently stabilised in nanoparticles compared to the essential oil of *Lippia grata*, showing smaller nanoparticle sizes and higher zeta potential values than the nanoparticles encapsulated with essential oil. The release profile of the active ingredients can be divided into two stages: a high initial release followed by a slower release. NC films with nanoparticles encapsulated with polyphenols showed better mechanical properties than films with nanoparticles encapsulated with essential oil.

Finally, it was evident that NP-OE was effective against the growth of *Lasiodiplodia theobromae*, highlighting that the formulation should be tested *in vivo* and has great potential in the active coating of fruits.

#### References

- Albuquerque, C.C., Camara, T.R., Mariano, R.L.R., Willadino, L., Marcelino Jr., C. and Ulisses, C. (2006) 'Antimicrobial action of the essential oil of *Lippia gracilis* Schauer', *Braz. Arch. Biol. Technol.*, Vol. 49, No. 4, pp.527–535 [online] <https://doi.org/10.1590/S1516-89132006000500001>.
- Antoniou, J., Liu, F., Majeed, H. and Zhong, F. (2015) 'Characterization of tara gum edible films incorporated with bulk chitosan and chitosan nanoparticles: a comparative study', *Food Hydrocoll.*, Vol. 44, pp.309–319 [online] <https://doi.org/10.1016/j.foodhyd.2014.09.023>.
- ASTM E96/E95M (1995) *Standard Test Methods for Water Vapor Transmission of Materials*.
- Azereido, H.M.C. (2009) 'Nanocomposites for food packaging applications', *Food Res. Int.*, Vol. 42, No. 9, pp.1240–1253 [online] <https://doi.org/10.1016/j.foodres.2009.03.019>.
- Bakkali, F., Averbeck, S., Averbeck, D. and Idaomar, M. (2008) 'Biological effects of essential oils – a review', *Food Chem. Toxicol.*, Vol. 46, pp.446–475 [online] <https://doi.org/10.1016/j.fct.2007.09.106>.
- Barzegar, M., Ghahfarokhi, M.G., Sahari, M.A. and Azizi, M.H. (2016) 'Enhancement of thermal stability and antioxidant activity of thyme essential oil by encapsulation in chitosan nanoparticles', *J. Agric. Sci. Technol.*, Vol. 18, No. 7, pp.1781–1792 [online] <http://jast.modares.ac.ir/article-23-9470-en.html>.
- Britto, D., Moura, M.R., Aouada, F.A., Mattoso, L.H.C. and Assis, O.B.G. (2012) 'N, N, N-trimethyl chitosan nanoparticles as a vitamin carrier system', *Food Hydrocoll.*, Vol. 27, pp.487–493 [online] <https://doi.org/10.1016/j.foodhyd.2011.09.002>.
- Britto, D., Moura, M.R., Aouada, F.A., Pinola, F.G., Lundstedt, L.M., Assis, O.B.G. and Mattoso, L.H.C. (2014) 'Entrapment characteristics of hydrosoluble vitamins loaded into chitosan and N, N, N-trimethyl chitosan nanoparticles', *Macromol. Res.*, Vol. 22, pp.1261–1267 [online] <https://doi.org/10.1007/s13233-014-2176-9>.

- Bulmer, C., Margaritis, A. and Xenocostas, A. (2012) 'Production and characterization of novel chitosan nanoparticles for controlled release of rHuErythropoietin', *Biochem. Eng. J.*, Vol. 68, pp.61–69 [online] <https://doi.org/10.1016/j.bej.2012.07.007>.
- Carvalho, R.R.C., Laranjeira, D., Carvalho Filho, J.L.S., Souza, P.E., Blank, A.F., Alves, P.B., Jesus, H.C.R. and Warwick, D.R.N. (2013) 'In vitro activity of essential oils of *Lippia sidoides* and *Lippia gracilis* and their major chemical components against *Thielaviopsis paradoxa*, causal agent of stem bleeding in coconut palms', *Química Nova*, Vol. 36, No. 2, pp.241–244 [online] <https://doi.org/10.1590/S0100-40422013000200007>.
- Cerqueira, M.A., Bourbon, A.I., Pinheiro, A.C., Martins, J.T., Souza, B.W.S., Teixeira, J.A. and Vicente, A.A. (2011) 'Galactomannans use in the development of edible films/coatings for food applications', *Trends Food Sci. Technol.*, Vol. 22, No. 12, pp.662–671 [online] <https://doi.org/10.1016/j.tifs.2011.07.002>.
- Cerqueira, M.A., Souza, B.W.S., Teixeira, J.A. and Vicente, A.A. (2012) 'Effect of glycerol and corn oil on physicochemical properties of polysaccharide films – a comparative study', *Food Hydrocoll.*, Vol. 27, No. 1, pp.175–184 [online] <https://doi.org/10.1016/j.foodhyd.2011.07.007>.
- Cruz-Valenzuela, M.R., Carrasco-Lugo, D.K., Vega-Vega, V., Gonzalez-Aguilar, G.A. and Ayala-Zavala, J.F. (2013) 'Fresh-cut orange treated with its own seed by-products presented higher antioxidant capacity and lower microbial growth', *Int. J. Postharvest Technol. Innovation*, Vol. 3, No. 1, pp.13–27 [online] <https://doi.org/10.1504/IJPTI.2013.051987>.
- Duarte, D.S., Nascimento, J.A.A. and Britto, D. (2019) 'Scale-up in the synthesis of nanoparticles for encapsulation of agroindustrial active principles', *Ciência e Agrotecnologia*, Vol. 43, p.e023819 [online] <http://dx.doi.org/10.1590/1413-7054201943023819>.
- Friedman, M. (2014) 'Antibacterial, antiviral, and antifungal properties of wines and winery byproducts in relation to their flavonoid content', *J. Agric. Food Chem.*, Vol. 62, No. 26, pp.6025–6042 [online] <https://doi.org/10.1021/jf501266s>.
- Gan, Q. and Wang, T. (2007) 'Chitosan nanoparticle as protein delivery carrier-Systematic examination of fabrication conditions for efficient loading and release', *Colloids Surf B Biointerfaces*, Vol. 59, No. 1, pp.24–34 [online] <https://doi.org/10.1016/j.colsurfb.2007.04.009>.
- Hadidi, M., Pouramin, S., Adinepour, F., Haghani, S. and Jafari, S.M. (2020) 'Chitosan nanoparticles loaded with clove essential oil: characterization, antioxidant and antibacterial activities', *Carbohydr. Polym.*, Vol. 236, Article No. 116075 [online] <https://doi.org/10.1016/j.carbpol.2020.116075>.
- Hasheminejad, N., Khodaiyan, F. and Safari, M. (2019) 'Improving the antifungal activity of clove essential oil encapsulated by chitosan nanoparticles', *Food Chem.*, Vol. 275, pp.113–122 [online] <https://doi.org/10.1016/j.foodchem.2018.09.085>.
- Hosseini, S.F., Zandi, M., Rezaei, M. and Farahmandghavi, F. (2013) 'Two-step method for encapsulation of oregano essential oil in chitosan nanoparticles: preparation, characterization, and in vitro release study', *Carbohydr. Polym.*, Vol. 95, pp.50–56 [online] <https://doi.org/10.1016/j.carbpol.2013.02.031>.
- Kavaz, D., Idris, M. and Onyebuchi, C. (2019) 'Physicochemical characterization, antioxidative, anticancer cells proliferation and food pathogens antibacterial activity of chitosan nanoparticles loaded with *Cyperus articulatus* rhizome essential oils', *Int. J. Biol. Macromol.*, Vol. 123, pp.837–845 [online] <https://doi.org/10.1016/j.ijbiomac.2018.11.177>.
- Kedia, A. and Dubey, N.K. (2018) 'Nanoencapsulation of essential oils: a possible way for an eco-friendly strategy to control postharvest spoilage of food commodities from pests', in Tripathi, D.K., Ahmad, P., Sharma, S., Chauhan, D.K. and Dubey, N.K. (Eds.): *Nanomaterials in Plants, Algae, and Microorganisms*, Chap. 22, pp.501–522, Academic Press [online] <https://doi.org/10.1016/B978-0-12-811487-2.00022-0>.

- Khalili, S.T., Mohsenifar, A., Beyki, M., Zhavah, S., Rahmani-Cherati, T., Abdollahi, A., Bayat, M. and Tabatabaei, M. (2015) 'Encapsulation of thyme essential oils in chitosan-benzoic acid nanogel with enhanced antimicrobial activity against *Aspergillus flavus*', *Food Sci. Technol.*, Vol. 60, No. 1, pp.502–508 [online] <https://doi.org/10.1016/j.lwt.2014.07.054>.
- Liang, J., Li, F., Fang, Y., Yang, W., An, X., Zhao, L., Xin, Z., Cao, L. and Hu, Q. (2011) 'Synthesis, characterization and cytotoxicity studies of chitosan-coated tea polyphenols nanoparticles', *Colloids Surf B Biointerfaces*, Vol. 82, No. 2, pp.297–301 [online] <https://doi.org/10.1016/j.colsurfb.2010.08.045>.
- López-Franco, Y.L., Cervantes-Montaño, C.I., Martínez-Robinson, K.G., Lizardi-Mendoza, J. and Robles-Ozuna, L.E. (2013) 'Physicochemical characterization and functional properties of galactomannans from mesquite seeds (*Prosopis spp.*)', *Food Hydrocoll.*, Vol. 30, No. 2, pp.656–660 [online] <https://doi.org/10.1016/j.foodhyd.2012.08.012>.
- Lorevice, M.V., Otoni, C.G., Moura, M.R. and Mattoso, L.H.C. (2016) 'Chitosan nanoparticles on the improvement of thermal, barrier, and mechanical properties of high- and low-methyl pectin films', *Food Hydrocoll.*, Vol. 52, pp.732–740 [online] <http://dx.doi.org/10.1016/j.foodhyd.2015.08.003>.
- Lu, Y., Weng, L. and Cao, X. (2005) 'Biocomposites of plasticized starch reinforced with cellulose crystallites from cottonseed linter', *Macromol. Biosci.*, Vol. 5, No. 11, pp.1101–1107 [online] <https://doi.org/10.1002/mabi.200500094>.
- Medeiros, B.G.D., Pinheiro, A.C., Cunha, M.G.C. and Vicente, A.A. (2012) 'Development and characterization of a nanomultilayer coating of pectin and chitosan – evaluation of its gas barrier properties and application on 'Tommy Atkins' mangoes', *J. Food Eng.*, Vol. 110, No. 3, pp.457–464 [online] <https://doi.org/10.1016/j.jfoodeng.2011.12.021>.
- Nascimento, J.A.A., Gomes, L.K.S., Duarte, D.S., Lima, M.A.C. and Britto, D. (2019) 'Stability of nanocomposite edible films based on polysaccharides and vitamin C from agroindustrial residue', *Mater. Res.*, Vol. 22, No. 3, p.e20190057 [online] <http://dx.doi.org/10.1590/1980-5373-MR-2019-0057>.
- Otoni, C.G., Moura, M.R., Aouada, F. and Camilloto, G.P. (2014) 'Antimicrobial and physical-mechanical properties of pectin/papaya puree/cinnamaldehyde nanoemulsion edible composite films', *Food Hydrocoll.*, Vol. 41, pp.188–194 [online] <https://doi.org/10.1016/j.foodhyd.2014.04.013>.
- Paula, H.C.B., Sombra, F.M., Abreu, F.O.M.S. and Paul, R.C.M. (2010) 'Lippia sidoides essential oil encapsulation by angico gum/chitosan nanoparticles', *J. Braz. Chem. Soc.*, Vol. 21, No. 12, pp.2359–2366 [online] <https://doi.org/10.1590/S0103-50532010001200025>.
- Peixinho, G.S., Ribeiro, V.G. and Amorim, E.P.R. (2017) 'Controle da Podridão seca (*Lasiodiplodia theobromae*) em cachos de videira cv. Itália por óleos essenciais e quitosana', *Summa Phytopathologica*, Vol. 43, No. 1, pp.26–31 [online] <https://doi.org/10.1590/0100-5405/2201>.
- Picard, I., Hollingsworth, R.G., Wall, M., Nishijima, K., Salmieri, S., Vu, K.D. and Lacroix, M. (2013) 'Effects of chitosan-based coatings containing peppermint essential oil on the quality of post-harvest papaya fruit', *Int. J. Postharvest Technol. Innovation*, Vol. 3, No. 2, pp.178–189 [online] <https://doi.org/10.1504/IJPTI.2013.055845>.
- Sae-Tang, N., Thompson, A.K. and Puttongsiri, T. (2020) 'Prolonging the postharvest life of fresh mangoes with a combination of edible coatings', *Int. J. Postharvest Technol. Innovation*, Vol. 7, No. 3, pp.171–183 [online] <https://doi.org/10.1504/IJPTI.2020.110412>.
- Silva, C.B., Duarte, D.S., Souza, A.V., Assis, O.B.G. and Britto, D. (2020) 'Synthesis of chitosan polysaccharide nanoparticles for skin grape extract stabilization', *Braz. J. Dev.*, Vol. 6, No. 4, pp.17913–17930 [online] <https://doi.org/10.34117/bjdv6n4-094>.

- Souza Filho, M.S.M., Nascimento, R.M., Cavalcante, F.L., Rosa, M.F., Morais, J.P.S., Feitosa, J.P.A., Melo, E.F., Cruz, M.R. and Alexandre, L.C. (2013) *Extração e Caracterização de Galactomanana de Vagens de Algaroba (Prosopis juliflora)*, Embrapa Agroindústria Tropical, Fortaleza.
- Souza, A.V., Santos, U.S., Corrêa, R.M., Souza, D.D. and Oliveira, F.J.V. (2017) 'Essential oil content and chemical composition of *Lippia gracilis* Schauer cultivated in the sub-meddle São Francisco Valley', *J. Essential Oil Bearing Plants*, Vol. 20, No. 4, pp.983–994 [online] <http://dx.doi.org/10.1080/0972060X.2017.1377117>.
- Taludher, R. and Shivakumar, K. (2013) 'Tensile properties of veins of damselfly wing', *J. Biomater. Nanobiotechnol.*, Vol. 4, pp.247–255 [online] <https://doi.org/10.4236/jbnb.2013.43031>.